

Effects of Ce, Mo and Si ion implantation on the passive layer composition and high-temperature oxidation behaviour of AISI 304 stainless-steel studied by soft x-ray absorption spectroscopy

A. Gutiérrez,^{1*} M. F. López,² F. J. Pérez Trujillo,³ M. P. Hierro³ and F. Pedraza³

¹ Departamento de Ciencia y Tecnología de Materiales, Universidad Miguel Hernández, Avda Ferrocarril s/n, E-03202 Elche, Spain

² Ingeniería de Materiales, Degradación y Durabilidad, Centro Nacional de Investigaciones Metalúrgicas, Avda. Gregorio del Amo 8, E-28040 Madrid, Spain

³ Departamento de Ciencia de Materiales, Universidad Complutense de Madrid, Spain

The influence of Ce, Mo and Si ion implantation on the chemical properties of AISI 304 stainless-steel passive and oxide layers was studied by means of soft x-ray absorption spectroscopy (XAS). Applying this technique at the transition metal 2p absorption thresholds, the composition and chemical state of the passive layer were determined. A surface Cr enrichment is observed for the ion-implanted samples in comparison with non-implanted samples, which can be associated with better corrosion behaviour. To investigate the effects of ion implantation on the high-temperature oxidation behaviour of AISI 304 stainless-steel, the oxide layer formed after an isothermal oxidation at 1173 K for 32 h was also investigated. The XAS data show mainly the presence of Cr and Mn oxides in the surface region of all samples. The Cr/Fe ratio—a parameter that can be associated with the protective character of the oxide scale—is higher for the Si- and Ce-implanted samples than for the as-received sample. The Mo-implanted sample has the lowest Cr/Fe ratio, suggesting a poor oxidation resistance at high temperatures in this case. Copyright © 2000 John Wiley & Sons, Ltd.

KEYWORDS: x-ray absorption spectroscopy; stainless-steel; ionic implantation; high-temperature oxidation; corrosion resistance

INTRODUCTION

Stainless-steels have found widespread use because of their good properties/price ratio. The term 'stainless' is associated with their chromium content, which, upon reaction with oxygen from the surrounding environment, renders a protective chromia film on the surface.¹ The properties of this passive film, as adherence and stability, determine the corrosion resistance of these materials.^{2–4} Much work has been devoted to modifying these passive layers by adding small amounts of some reactive elements at the surface to improve their corrosion behaviour. These so-called reactive elements (RE) are typically Y, Hf and some lanthanide elements that are readily oxidized at room temperature, and they can give rise to perovskite-like oxides (ABO₃, with A = RE and B = Cr) within the passive layer at higher temperatures.⁵

Among the surface modification techniques, ion implantation presents several advantages: no high temperatures are needed, the bulk material remains unaffected after the implantation process, and the surface to be modified can be tailored by controlling the accelerating potential and the implanted dose.⁶ The ion fluences needed for surface modification of metals and alloys are usually quite low

(of the order of 10¹⁶–10¹⁸ ions cm⁻² to increase corrosion resistance, and 10¹⁴–10¹⁶ ions cm⁻² to improve wear and erosion⁷), which results in a commercially feasible process for the production of tools.⁸

The changes introduced at the material surface by ion implantation and its effects on the corrosion behaviour of materials can be evaluated by investigating the chemical composition of their surface. In a recent work, Auger electron spectroscopy (AES) was used to determine the presence of implanted species at the steel surface.⁹ However, the chemical composition of the passive layer was not evaluated completely because of the excessively high surface sensitivity of AES. On the other hand, x-ray absorption spectroscopy (XAS) measured in total electron yield (TEY) mode is a particularly suitable technique to study the chemical state of the different species at the passive layer. The absorption cross-section is measured by detecting all electrons escaping from the surface after decay of the core hole. The probing depth is of the order of 70–100 Å for transition metal 2p edges,¹⁰ which is very close to the passive layer thickness. In this work we apply this technique at the transition metal 2p edges in TEY mode to determine the composition of the passive layer of AISI 304 stainless-steel with and without Si, Mo and Ce ion implantation. Also, the composition of the oxide scale after oxidation at 1173 K for 32 h in both implanted and non-implanted samples is determined and compared with the passive layer formed spontaneously at room temperature.

* Correspondence to: A. Gutiérrez, Departamento de Ciencia y Tecnología de Materiales, Universidad Miguel Hernández, Avda Ferrocarril s/n, E-03202 Elche, Spain.
E-mail: ale@umh.es

EXPERIMENTAL

The chemical composition of the AISI 304 stainless-steel investigated is (wt.%): 18.2 Cr, 9.4 Ni, 1.5 Mn, 0.4 Si, 0.2 Mo, 0.2 Cu, 0.1 Co, 0.047 C, 0.027 P, 0.005 N, 0.003 S, 0.003 Ti, 0.002 Al and remainder Fe. The AISI 304 samples were implanted using an accelerating potential of 150 keV up to ion doses of (ions cm^{-2}) 1×10^{15} Si, 1×10^{14} Mo and 1×10^{14} Ce. Oxidation of both implanted and non-implanted specimens was carried out in a muffle furnace at 1173 K and at atmospheric pressure of air for different times up to 144 h.

The AISI stainless-steel samples were studied as-received and after Mo, Ce and Si ionic implantation, both before and after high-temperature oxidation. As reference materials, Fe, Cr and Ni pure metal polycrystalline samples, as well as FeO, oxidized Fe and oxidized Cr samples, were also investigated. The pure metal samples were scraped *in situ* in the ultrahigh vacuum (UHV) chamber with a diamond file. Both Fe and Cr oxidized samples were produced by air exposure, generating spontaneously a native oxide layer on each sample surface. The FeO was also scraped *in situ* in the UHV chamber with a diamond file to remove surface contaminants.

The XAS measurements were carried out at the SX700/I soft x-ray monochromator at the Berliner Elektronenspeicherring für Synchrotronstrahlung (BESSY). The XAS spectra were obtained by recording the total yield of secondary electrons from the sample surfaces. The base pressure in the UHV chamber during measurements was better than 2×10^{-10} mbar.

RESULTS

Figure 1(a) represents the Fe 2p soft x-ray absorption spectra of all AISI 304 stainless-steel samples as-received and after Si, Mo and Ce ionic implantation, as well as Fe metal and FeO for comparison. The different peak shapes obtained for the AISI 304 samples indicate that the ionic implantation process produces chemical changes in the outer region of the material. The Fe 2p spectrum of the as-received AISI 304 sample is similar to that of FeO except for the presence of a shoulder at ~ 708 eV. This effect can be assigned to a small amount of Fe_2O_3 , as can be deduced by comparing with the Fe_2O_3 spectrum of previous works.¹¹ This would increase the spectral weight at ~ 708 eV. Because FeO evolves towards Fe_2O_3 in contact with oxygen, its presence is limited to the internal region of the passive layer, at the interface between it and the metallic substrate. The Fe 2p spectrum of the Si-implanted AISI 304 sample, however, exhibits the typical features of Fe metal, suggesting that the Fe signal is coming mainly from the substrate and that no Fe oxides are present in the passive layer. On the other hand, the shape of the Fe 2p Mo-implanted AISI 304 signal is rather different to the other AISI 304 samples. This shape is typical of Fe_3O_4 ,¹¹ suggesting the formation of this oxide in the passive layer. Finally, the Fe 2p Ce-implanted AISI 304 spectrum exhibits mainly the presence of Fe metal coming from the substrate, as can be deduced from its similarity with the Fe metal signal. However, the peak shape is slightly broader with a more pronounced spectral feature at ~ 708 eV, which may be assigned to a small amount of Fe oxide.

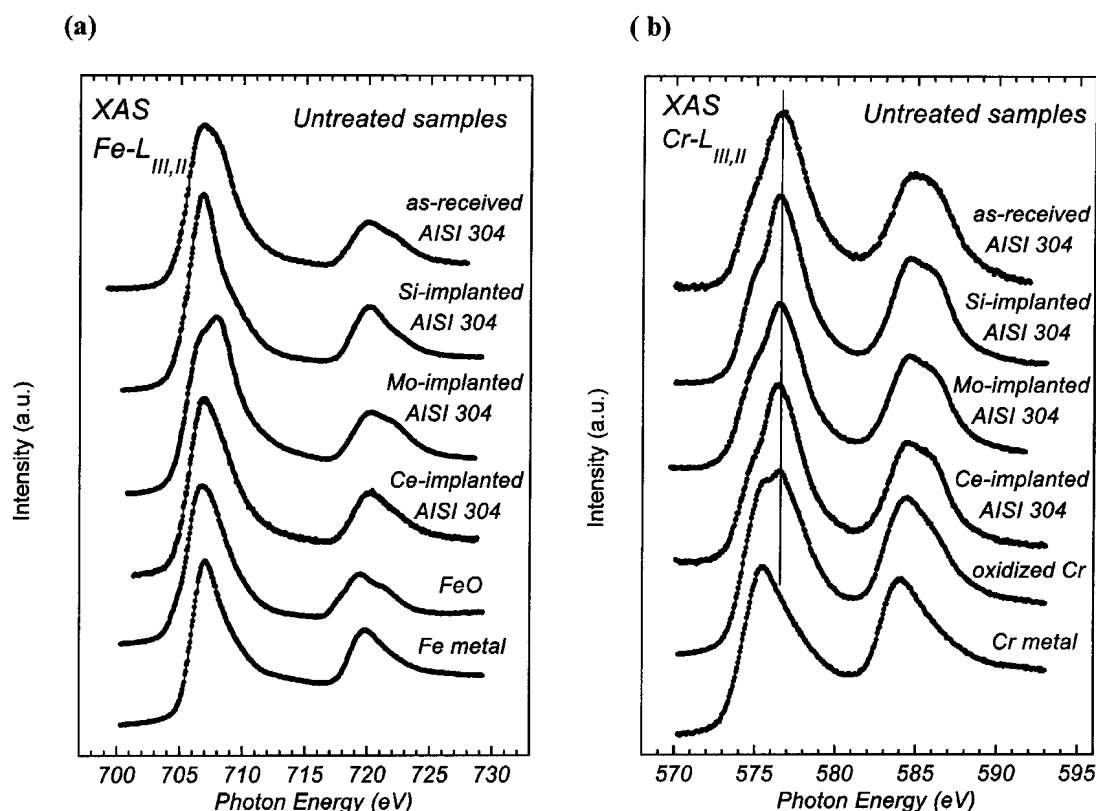


Figure 1. (a) Iron 2p soft x-ray absorption spectra of as-received AISI 304 stainless-steel, Si-, Mo-, and Ce-implanted AISI 304 stainless-steel, Fe metal and FeO. (b) Chromium 2p soft x-ray absorption spectra of as-received AISI 304 stainless-steel, Si-, Mo-, and Ce-implanted AISI 304 stainless-steel, oxidized Cr and Cr metal.

Figure 1(b) shows the Cr 2p soft x-ray absorption spectra of all AISI 304 stainless-steel samples as well as oxidized Cr and metallic Cr for comparison. The typical shape of the Cr₂O₃ soft x-ray absorption spectrum exhibits in the 2p_{3/2} region a main peak at ~576.5 eV and a distinctive shoulder located at ~575.5 eV.¹¹ The spectrum of Cr metal has a different shape to that of Cr₂O₃, with a main peak located at ~575.5 eV. The oxidized Cr spectrum that corresponds to the native oxide film shows a mixture of metallic chromium and Cr₂O₃. As the metallic contribution increases, the intensity of the shoulder at ~575.5 eV also increases. The spectrum of the Si-implanted AISI 304 sample exhibits the spectral feature corresponding to the shoulder at ~575.5 eV more clearly defined than all other samples. This indicates that the spectral width of both peaks—shoulder and main structure—is smaller for the Si-implanted AISI 304 sample than for the other samples, suggesting that in this case the structure of the Cr₂O₃ is not modified.¹¹ On the other hand, the Cr 2p signal of the Mo-implanted, Ce-implanted and as-received AISI 304 samples has broader structures. This result suggests a modification of the primary Cr₂O₃ oxide structure in these samples. The Cr 2p Mo-implanted AISI 304 spectrum shows the broadest 2p_{3/2} structure with the highest shoulder intensity. The latter indicates a higher metallic content, which can be associated with a thinner passive layer compared to all other AISI 304 samples.

Owing to the high interest in stainless steels for intermediate and high-temperature applications, it is important to characterize the outer layer of these materials after performing a heat treatment. Figure 2 shows the composition percentage corresponding to the as-received, Si-implanted, Ce-implanted and Mo-implanted AISI 304 stainless steels after oxidation at 1173 K for 32 h. The values represented in this graph were obtained from the XAS spectra corresponding to the different absorption edges. The high-temperature oxidation leads to Cr and Mn enrichment in the oxide scale, which suggests the formation of Cr–Mn oxides. This result agrees with conventional x-ray diffraction data, as shown in Fig. 3, where Mn_{1.5}Cr_{1.5}O₄ spinel-type oxides were identified together with some amount of Cr_{1.3}Fe_{0.7}O₃ oxides.

An important parameter in determining the corrosion resistance of steels is the Cr/Fe ratio in the oxide layer, because a higher value of this parameter is associated with a higher oxidation resistance. In Fig. 4, the values of the Cr/Fe ratio for all samples both before and after

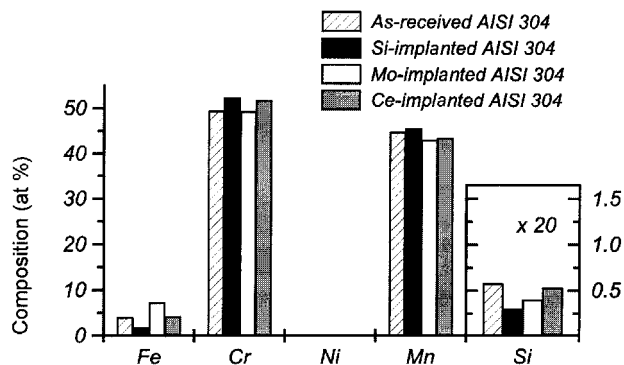


Figure 2. Chemical composition (in at.%) of the surface region of as-received and ion-implanted AISI 304 stainless-steel after oxidation at 1173 K for 32 h, obtained from the XAS spectra corresponding to the different absorption edges.

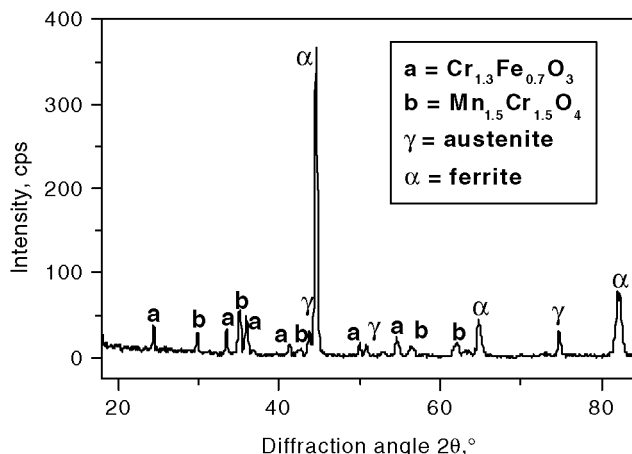


Figure 3. X-ray diffractogram obtained after 32 h of oxidation in air at 1173 K on the Si-implanted AISI 304 stainless-steel sample.

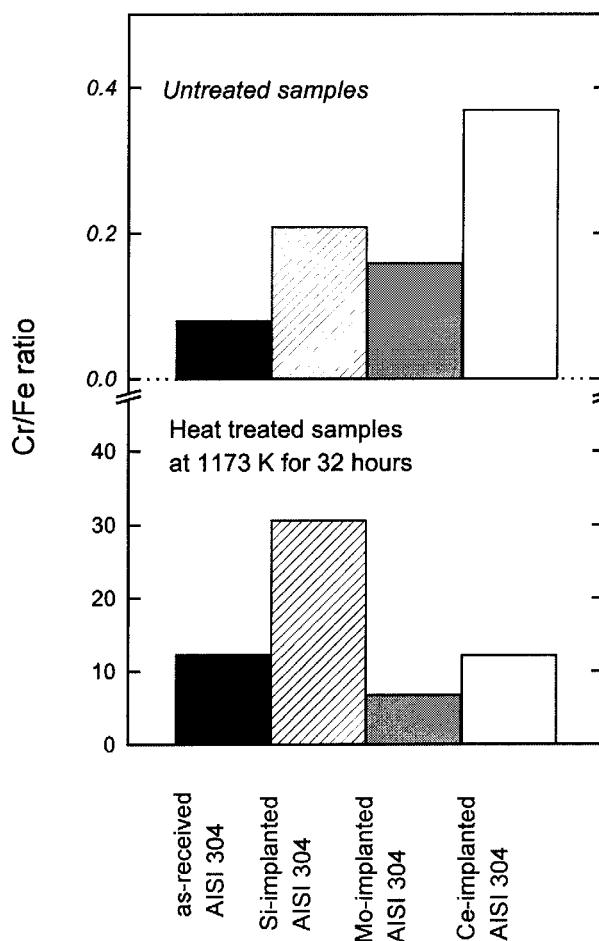


Figure 4. The Cr/Fe ratio derived from the corresponding XAS spectra of as-received and ion-implanted samples both before and after oxidation at 1173 K for 32 h.

high-temperature oxidation are shown. In the first case, all implanted specimens present a higher Cr/Fe ratio than the as-received steel sample, suggesting a higher corrosion resistance. However, the oxidized specimens show a different trend. As can be observed in Fig. 4, the Mo-implanted sample has a lower Cr/Fe ratio than all other samples, even the non-implanted sample. Consequently, Mo implantation on steels can lead to a linear oxidation behaviour at high temperatures (1173 K). On the other

hand, Si-implanted samples show the highest Cr/Fe ratio, whereas Ce-implanted samples achieve a similar value to non-implanted steel. These results emphasize the different corrosion resistance of the different materials at room temperature and at elevated temperatures.

The results shown in Fig. 4 are confirmed by the oxidation kinetics curves plotted in Fig. 5. It can be seen readily that the Mo-implanted steel undergoes approximately linear kinetics upon oxidation in air at 1173 K, probably due to the formation of volatile molybdenum oxides such as MoO_2 and MoO_3 at high temperatures.¹² A larger grain size and an open morphology are the main features of the Mo-implanted AISI 304 oxide scale after 144 h of exposure compared to that observed on the Ce-implanted steel (Fig. 6). This leads to catastrophic oxidation of the steel because the mass gain increases linearly with time. The higher Cr/Fe ratio found for the Si-implanted steel explains its higher mass gain at the first stages of oxidation, giving rise to the formation of a protective oxide scale composed of $(\text{Cr,Fe})_2\text{O}_3$ and $(\text{Mn,Cr})_2\text{O}_4$ (see Fig. 3). Once this oxide

scale is established, the kinetics change dramatically from linear to parabolic. Although this Cr/Fe ratio is similar for both the as-received and the Ce-implanted steels, the mass gain of the implanted specimens is higher due to the fact that, as mentioned above, cerium is oxidized very rapidly. After a short time, cerium might play a key role in the oxide scale grown at high temperature.

From our results, the effects of ion implantation are different for different temperatures. At room temperature, ion implantation increases the chromium content of the passive layer in all cases (Si, Mo, and Ce), which will result in an improvement of the corrosion performance. This enrichment in chromium will, accordingly, enhance the protective behaviour of the oxide scales after high-temperature oxidation in the case of Si and Ce implantation. In the case of Mo implantation, the volatile character of molybdenum oxides at temperature above 873 K will result in the formation of less-protective oxides, rich in Fe_3O_4 , which in turn will not be able to support high-temperature oxidation resistance.

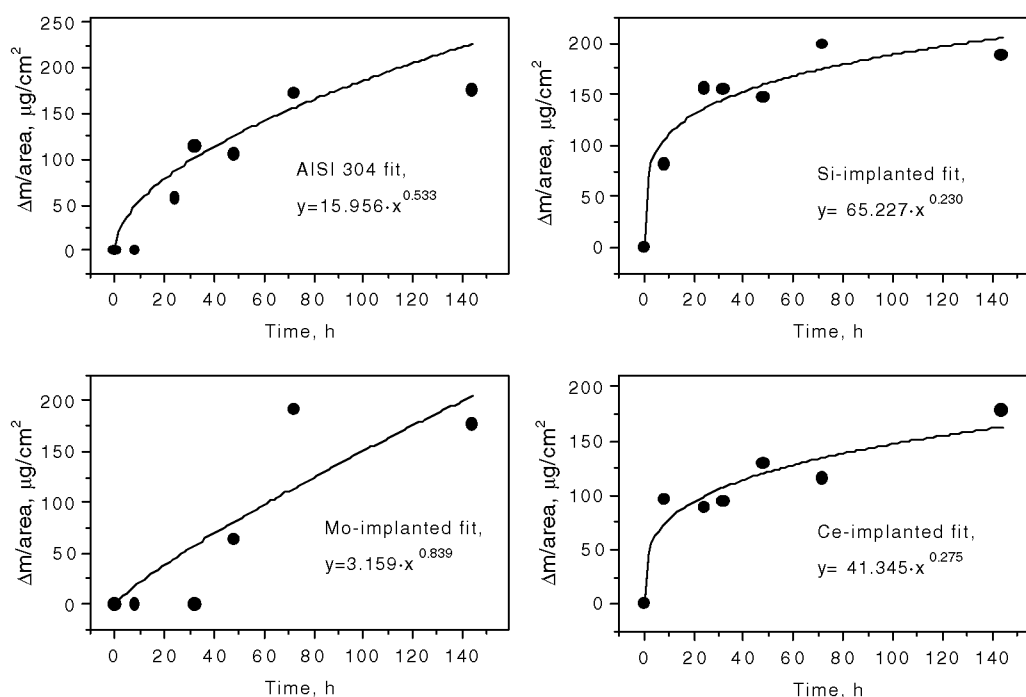


Figure 5. Experimental and kinetic laws, obtained by a least-squares fit, of non-implanted and implanted AISI 304 stainless steel after 144 h of oxidation in air at 1173 K.

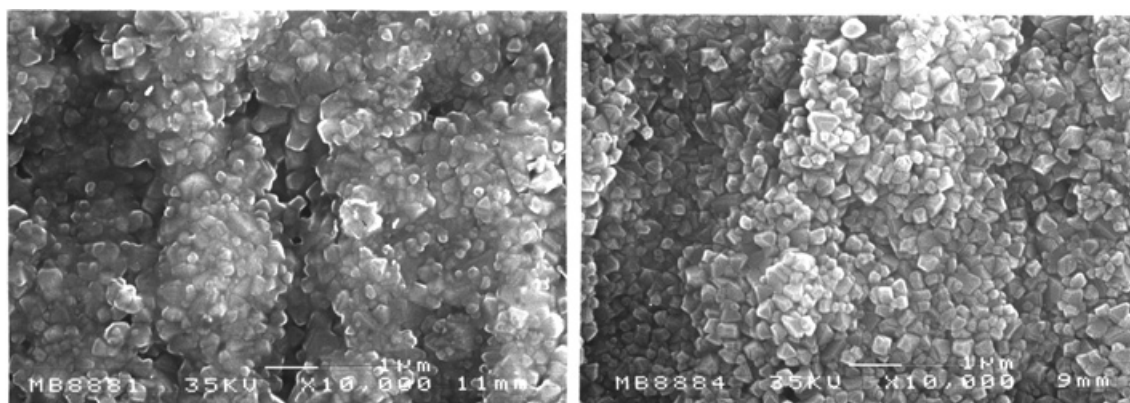


Figure 6. Scanning electron microscopy images of the oxide scales of the Mo-implanted sample (a) and the Ce-implanted sample (b) after oxidation at 1173 K for 32 h.

REFERENCES

1. Kane RD. *Adv. Mater. Process.* 1993; **7**: 16.
2. Bastidas JM, López MF, Gutiérrez A, Torres CL. *Corros. Sci.* 1998; **40**: 431.
3. López MF, Gutiérrez A, Torres CL, Bastidas JM. *J. Mater. Res.* 1999; **14**: 763.
4. Moon DP, Bennett MJ. *Mater. Sci. Forum.* 1989; **43**: 269.
5. Saito Y, Ónay B, Maruyama T. *J. Phys. IV Coll. C9* 1993; **3**: 217.
6. Townsend J. *J. Contemp. Phys.* 1987; **27**: 241.
7. Iskanderova A, Radhabov TD, Rakhimova GR. *Phys. Chem. Mech. Surf.* 1984; **8**: 1081.
8. Straede CA, Mikkelsen NJ. *Surf. Coat. Technol.* 1996; **84**: 567.
9. Pérez FJ, Otero E, Hierro MP, Gómez C, Pedraza F, de Segovia JL, Román E. *Surf. Coat. Technol.* 1998; **108/109**: 127.
10. Abbate M, Goedkoop JB, de Groot FMF, Grioni M, Fuggle JC, Hofmann S, Petersen H, Sacchi M. *Surf. Interface Anal.* 1992; **18**: 65.
11. Soriano L, Abbate M, de Groot FMF, Alders D, Fuggle JC, Hofmann S, Petersen H, Braun W. *Surf. Interface Anal.* 1993; **20**: 21.
12. Grabke HJ, Meier GH. *Oxid. Met.* 1995; **38**: 147.